Project Title: Crystal Preparation of Ni-Mn-Ga Alloys

Final Report

Submitted to: Office of Naval Research

by

Institute for Physical Research and Technology
Iowa State University
Ames, Iowa 50011

Principal Investigator: Thomas A. Lograsso, Senior Scientist
Materials Science and Engineering Department
Institute for Physical Research and Technology
Iowa State University
(515) 294-8425
lograsso@ameslab.gov

Co-Workers: Deborah L. Schlagel, Assistant Scientist
Wei Zhang, Graduate Student
Yi Lei Wu, Graduate Student

Project Period: August 1, 1999 - December 31,1999

Funding Level: $ 40,878

Endorsements:

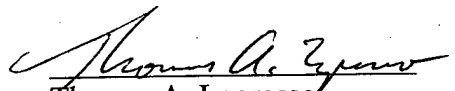

Thomas A. Lograsso
Senior Scientist
(515) 294-8425

REPORT DOCUMENTATION PAGE

Form Approved
OMB No. 0704-0188

1. REPORT DATE *(DD-MM-YYYY)*	2. REPORT DATE	3. DATES COVERED *(From - To)*
31-01-2000	Final Technical Report	01 AUG 99 to 31 DEC 00

4. TITLE AND SUBTITLE

Crystal Preparation of Ni-Mn-Ga Alloys

5a. CONTRACT NUMBER

5b. GRANT NUMBER

N00014-99-1-0997

5c. PROGRAM ELEMENT NUMBER

6. AUTHOR(S)

Thomas Lograsso

5d. PROJECT NUMBER

99PR07890-00

5e. TASK NUMBER

5f. WORK UNIT NUMBER

7. PERFORMING ORGANIZATION NAME(S) AND ADDRESS(ES)

Iowa State University

8. PERFORMING ORGANIZATION REPORT NUMBER

9. SPONSORING/MONITORING AGENCY NAME(S) AND ADDRESS(ES)

Office of Naval Research
ONR 332
Ballston Centre Tower One, 800 N Quincy St
Arlington, VA 22217-5660

10. SPONSOR/MONITOR'S ACRONYM(S)

ONR

11. SPONSORING/MONITORING AGENCY REPORT NUMBER

12. DISTRIBUTION AVAILABILITY STATEMENT

Approved for Public Release; Distribution is Unlimited

13. SUPPLEMENTARY NOTES

14. ABSTRACT

Partial evaluation of the liquidus diagram of Ni-Mn-Ga by thermal analysis and microstructural evaluation has determined that the primary solidification surface for the Heusler alloy phase exists over a wide range of compositions. The primary solidification surface falls modestly in temperature with either increasing Mn or Ga concentrations. The composition, $Ni_{50}Mn_{25}Ga_{25}$, melts incongruently over a temperature range of approximately 18°C. The small temperature range of solidification allows for the conditions suitable for crystal growth to be easily established and maintained throughout the crystal growth process for a wide variety of compositions. In general, the Mn composition increases as the solid grows with an associated decrease in Ni composition. Analysis of the composition profiles indicated that the compositional changes, and hence, the solidification process, is dominated by convective mixing in the liquid during growth and evaporative losses of Mn. Finally, preliminary experiments were conducted that demonstrated the feasibility of using the Czochralski technique for the preparation of Ni-Mn-Ga alloys. Additional process optimization is required to gain confidence in applying the Czochralski method to the routine preparation of $Ni_{50}Mn_{25}Ga_{25}$ and its alloys.

15. SUBJECT TERMS

Ferro magnetic, crystal growth, Ni-Mn-Ga, shape memory

16. SECURITY CLASSIFICATION OF:			17. LIMITATION OF ABSTRACT	18. NUMBER OF PAGES	19a. NAME OF RESPONSIBLE PERSON
a. REPORT	b. ABSTRACT	c. THIS PAGE			Thomas Lograsso
U	U	U	UU	15	19b. TELEPONE NUMBER *(Include area code)* 515-294-8425

Objectives

The focus of the work conducted in this study concentrated on elucidating various aspects of the liquid-solid phase equilibria of the Ni-Mn-Ga alloy system and to apply this knowledge to improvements in the processing and preparation of single crystals of $Ni_{50}Mn_{25}Ga_{25}$. This work focused on three areas of study: partial elaboration of the liquidus surface of the Ni-MnGa system, characterization of compositional profiles known to exist in Bridgman prepared single crystal and development of Czochralski growth technique to Ni-Mn-Ga alloys.

Background and Previous Work

Single crystals of a number of different alloy compositions in the Ni-Mn-Ga alloy system have been prepared [1-3]. The studies have focused on property determination and characterization of the shape memory transformations and therefore did not require crystals of large dimensions and could easily be extracted from a large grain polycrystalline ingot. In all cases the single crystalline samples were prepared by the Bridgman method using a standard approach, the details of which are seldom given. There are no reports in the literature of preparation of large (several cm^3) single crystal by either the Bridgman method or other techniques.

Attempts to scale-up the crystal growth of Ni-Mn-Ga alloys in our laboratory using the Bridgman method has had limited success. We have attempted to prepare a number of different alloys including the stoichiometric $Ni_{50}Mn_{25}Ga_{25}$ (Wuttig–University of Maryland), off stoichiometric $Ni_{50}Mn_{30}Ga_{20}$ and $Ni_{50}Mn_{28}Ga_{22}$ (Wuttig–UM), a Ni-rich alloy (Inoue–University of Washington) and a Ni-deficient alloy (O'Handley-MIT). With the exception of the latter alloy, growth of these alloys has typically resulted in ingots containing a handful of crystals, elongated along the length of the ingot. On the other hand, crystal growth of the Ni-deficient alloy produced entire single crystals (1.5 cm diameter x 6 cm long) for the three crystal growth attempts to date. From a crystal growth standpoint, these results are somewhat surprising in that conventional wisdom holds that stoichiometric compositions (especially those that melt congruently) should be more amenable to growth of large crystals. Unfortunately, our involvement in the preparation of the alloys has been on a custom basis and investigation of this compositional effect could not be pursued.

Despite the success of preparing crystals of the Ni-deficient alloy, O'Handley has reported [4] that the composition of the crystal varies significantly along the length of the crystal and has a large effect on both the magnetic properties and shape memory transition temperatures. Unfortunately, compositional changes are a natural consequence of the directional solidification employed in the Bridgman method combined with the convection in the liquid during growth due to density differences from temperature and solutal variations. While compositional variations have not been measured for the other alloys, they have been qualitatively observed. Using a magnet, the difference in magnetic attraction found at each end of the ingot is profound. These compositional variations not only affect the magnetic properties but the transition temperatures of the shape memory transitions also vary along the length. This in turn will produce a non-uniform

magnetostrictive response along the length of the crystal. Clearly, a method of crystal preparation that would result in a more uniform composition profile is desired.

Work Plan

The work proposed under this grant focused first on the differences in the ability to prepare a single crystal from alloys of differing compositions in the Ni-Mn-Ga family. Previous studies have focused primarily on the low temperature phase equilibria, and very little is known about the solid-liquid phase equilibria in the area of interest in the Ni-Mn-Ga alloy system. We propose to elaborate the liquidus diagram for this region of the phase diagram through thermal analysis and DTA measurements of solidification. These temperature data will be correlated with the solidification microstructure to gain a complete understanding of the solidification events during solidification. Furthermore, the liquidus diagram will also provide information on the compositional and melting temperature changes during crystal growth.

Second, we will explore methods to reduce the compositional variations occurring during crystal growth. The rate at which the composition varies is a function of the overall length of ingot. We recently have acquired a Bridgman crystal growth furnace with a capacity to process an 8" long crucible, nearly double the previous capacity. While compositional gradients will exist, they will be spread over twice the length and, therefore, the rate of change in composition will be reduced. The compositional gradients will be measured using Energy Dispersive Spectroscopy compared with the profiles determined from smaller ingots.

Third, we will apply the Czochralski (CZ) technique to the growth of Ni-Mn-Ga alloys. The CZ method differs from the Bridgman in that a crystal is pulled from a melt whose volume is generally much larger than the crystal being prepared. Since less of the melt is solidified the changes in melt composition during growth is minimized. Maintaining the melt composition enables the composition of the crystal to be uniform over its length. An added advantage to the CZ method is that the growth can be seeded with a preferred orientation that will optimize the magnetostrictive response of the crystal. While the CZ method is more suited to producing uniform crystals it requires a higher degree of process control and operator - intervention than the Bridgman method. Given the information from the phase diagram will develop and optimize the processing conditions for CZ growth of Ni-Mn-Ga alloys.

Experimental Procedure

Phase Diagram Determination

Three pseudo-binary slices through the ternary system, as shown in Figure 1, were examined by thermal analysis to outline the primary solidification surface for the cubic Heusler $Ni_{50}Mn_{25}Ga_{25}$ phase. The pseudo-binary slices correspond to the following alloy series: $Ni_{50}Mn_{50-x}Ga_x$, $Ni_{100-2x}Mn_xGa_x$, $Ni_{2x}Mn_{100-3x}Ga_x$. The actual alloy compositions investigated within each pseudo-binary are given in Table 1.

Alloys were prepared by arc melting under an argon atmosphere using appropriate quantities of nickel (99.99% purity), manganese (99.9% purity) and gallium (99.99% purity) in thirty-gram lots. Thermal analysis was conducted in a graphite resistance heated furnace using calibrated Pt – Pt/Rh thermocouples. The thermocouples were calibrated to +/- 1 °C using the melting points of pure copper and pure gold. Alloys were placed in an alumina crucible and melted under argon atmosphere to a temperature between 50 and 100 °C above the melting point. The thermocouple was lowered into the center of the melt and repetitive cooling and heating cycles were performed at rates of 3.33 °C/sec. Following cycling the thermocouple was withdrawn and the alloy was cooled to room temperature at a controlled cooling rate. Microstructural examination and phase identification of the as-solidified structure were done using optical and electron microscopy coupled with chemical analysis using energy dispersive analysis (SEM-EDS). Samples for examination were prepared using standard metallographic techniques.

Compositional Variations during Bridgman Crystal Growth

High purity nickel, manganese and gallium were arc melted into buttons then drop cast into a chilled copper mold. Three different length ingots, standard, long and short, were prepared, weighing 73, 93.7 and 147 grams respectively. The nominal composition of these alloys was $Ni_{47.4}Mn_{32.1}Ga_{20.5}$. The as-cast ingots were placed in alumina crucibles (approximately 15 mm in diameter) and crystal growth was done in a Bridgman-style refractory metal resistance furnace. The sample was heated to 1350°C for 1 hr to allow homogenization before withdrawing the sample from the heat zone at a rate of 2.0 mm/hr. To minimize vaporization of the manganese during crystal growth, the furnace was backfilled to a positive pressure of 6.8×10^5 Pa with purified argon after the chamber and sample had been out gassed at 1350°C under vacuum. The as-grown crystal was sectioned longitudinally along the growth direction. Compositional variance both parallel to the growth direction and transverse to the growth direction was measured using SEM-EDS.

Crystal Growth by the Czochralski Method (CZ)

Seed crystals were prepared for the CZ method from Bridgman grown crystals as described in the previous section. The Bridgman crystals were oriented using Back-reflection Laue X-ray method to the [100] direction, the magnetic easy axis and section by spark machining into rods approximately 3 mm in diameter. The charge material for CZ was prepared by induction melting and chill casting a polycrystalline ingot, 25 mm in diameter and 300 mm long. Growth rates used during seed pulling range from 5 mm/hr to 15 mm/hour.

Table 1. Alloy compositions used in the determination of the primary solidification surface of the cubic $Ni_{50}Mn_{25}Ga_{25}$ Heusler phase.

$Ni_{50}Mn_{50-x}Ga_x$	$Ni_{100-2x}Mn_xGa_x$	$Ni_{2x}Mn_{100-3x}Ga_x$
$Ni_{50}Mn_{50}$	$Ni_{80}Mn_{10}Ga_{10}$	$Ni_{10}Mn_{85}Ga_5$
$Ni_{50}Mn_{40}Ga_{10}$	$Ni_{60}Mn_{20}Ga_{20}$	$Ni_{20}Mn_{70}Ga_{10}$
$Ni_{50}Mn_{30}Ga_{20}$	$Ni_{40}Mn_{30}Ga_{30}$	$Ni_{30}Mn_{55}Ga_{15}$
$Ni_{50}Mn_{25}Ga_{25}$	$Ni_{20}Mn_{40}Ga_{40}$	$Ni_{40}Mn_{40}Ga_{20}$
$Ni_{50}Mn_{20}Ga_{30}$	$Mn_{50}Ga_{50}$	$Ni_{60}Mn_{10}Ga_{30}$
$Ni_{50}Mn_{10}Ga_{40}$		Ni_2Ga_1
$Ni_{50}Ga_{50}$		

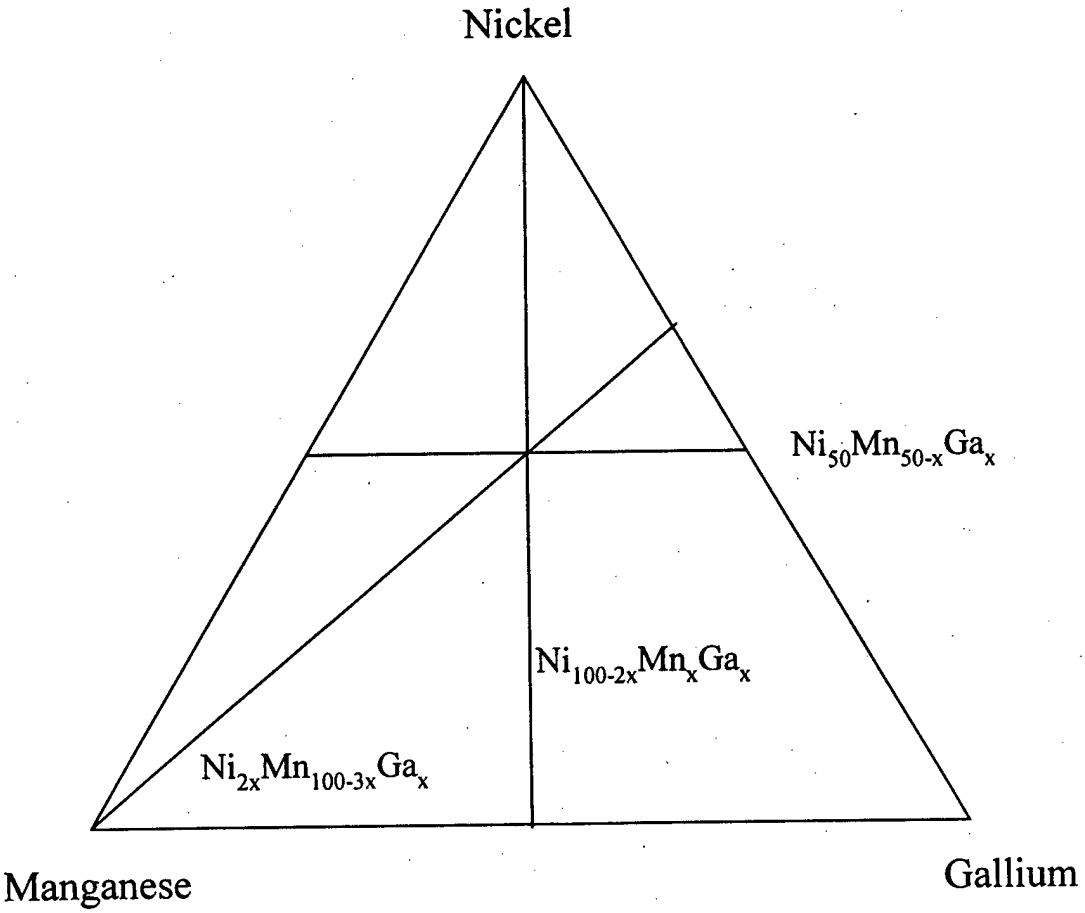

Figure 1 Pseudo-binary slices through the ternary Ni-Mn-Ga alloy system investigated in this work.

Results and Discussion

Phase Diagram Determination

The thermal analysis data of liquidus and solidus temperatures for the three alloy series investigated, $Ni_{50}Mn_{50-x}Ga_x$, $Ni_{100-2x}Mn_xGa_x$, $Ni_{2x}Mn_{100-3x}Ga_x$, are shown in Table 2-4 respectively. The stoichiometric composition of $Ni_{50}Mn_{25}Ga_{25}$ was found to melt non-congruently over a temperature range of approximately 20 °C. Figures 2-4 show the composition-temperature (C-T) curves (isopleths) of these three pseudo-binary slices. While a comprehensive determination of the solidification reactions and phase fields in each of these isopleths was beyond the limited scope of this study, the primary solidification fields were coarsely identified by changes in curvature of the measured liquidus curves coupled with the examination of the solidification microstructures. The primary solidification product for each alloy was identified metallographically and the composition determined by EDS. These results are summarized in Tables 2-4. The β phase ($Ni_{50}Mn_{25}Ga_{25}$) primary solidification field was found to exist over a large compositional range as illustrated in Figure 5.

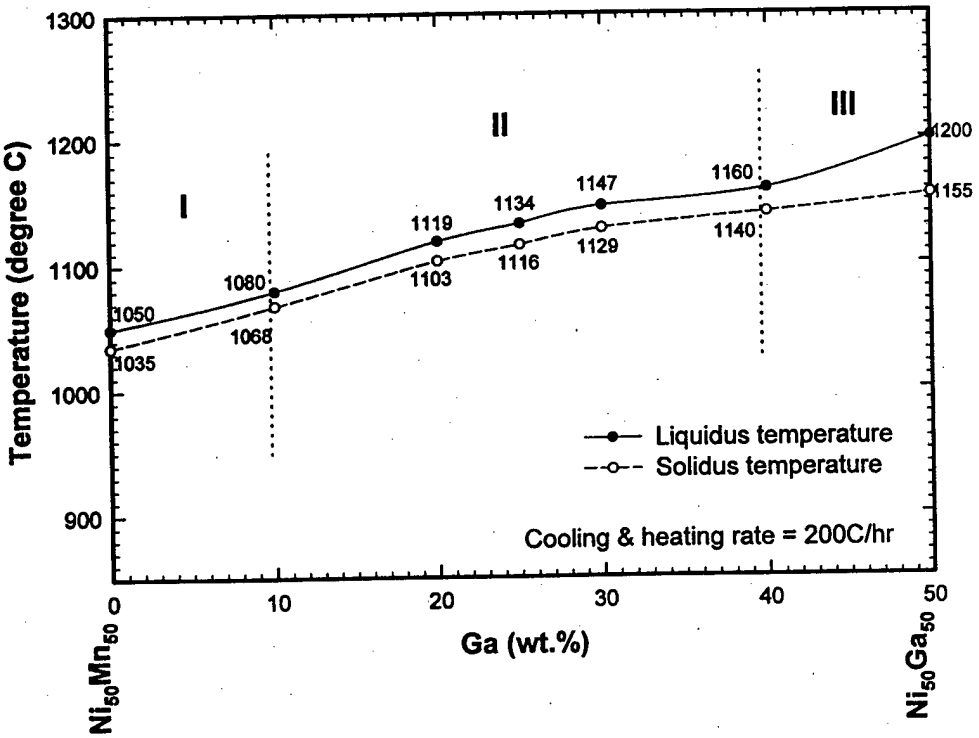

Figure 2 Composition-temperature isopleth for the $Ni_{50}Mn_{1-x}Ga_x$ alloy series.

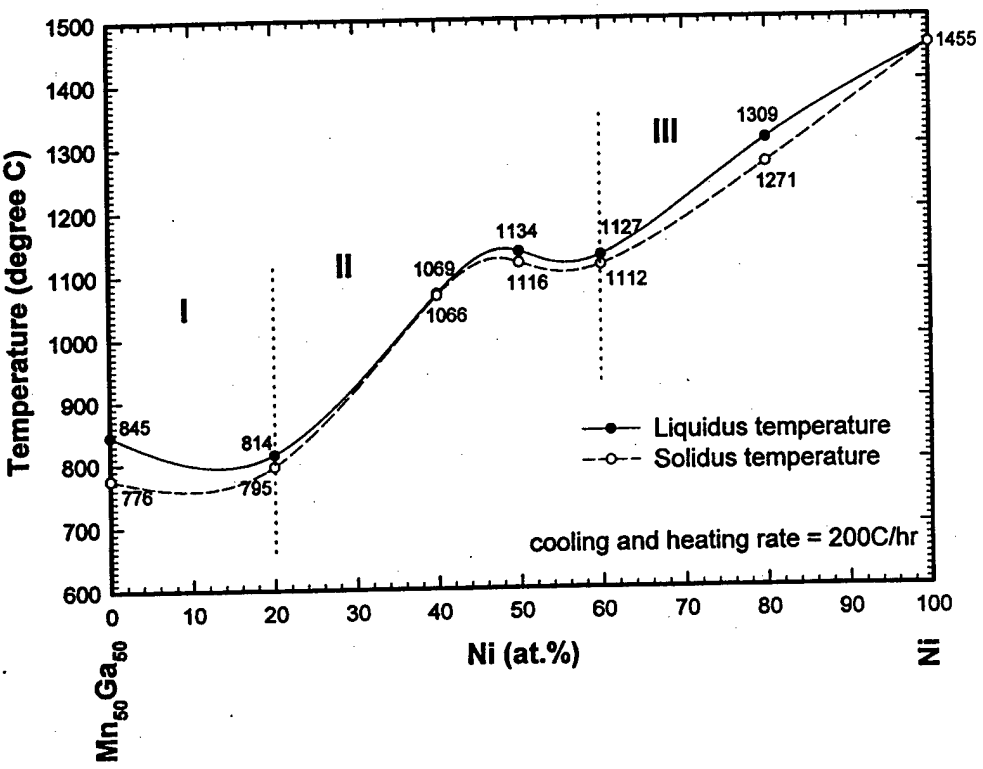

Figure 3 Composition-temperature isopleth for the $Ni_{100-2x}Mn_xGa_x$ alloy series.

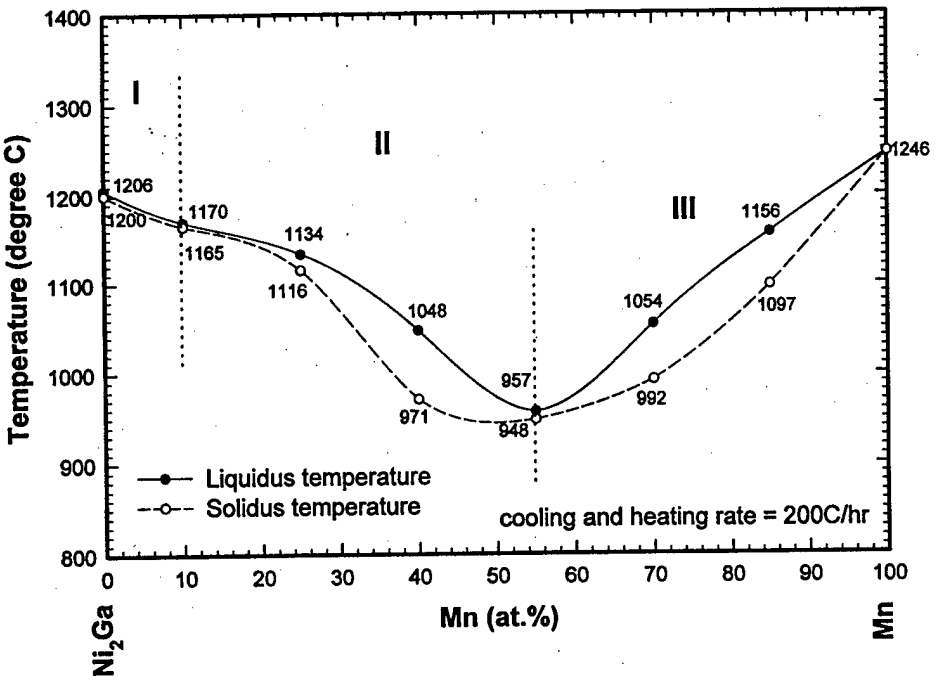

Figure 4 Composition-temperature isopleth for the $Ni_{2x}Mn_{100-3x}Ga_x$ alloy series.

Table 2. Thermal analysis data of $Ni_{50}Mn_{50-x}Ga_x$ alloys

	Liquidus (°C)	Solidus (°C)	Primary Solidification Product
$Ni_{50}Ga_{50}$	1200	1155	
$Ni_{50}Mn_{10}Ga_{40}$	1160	1140	α(fcc Ni)
$Ni_{50}Mn_{20}Ga_{30}$	1147	1129	β (B2)
$Ni_{50}Mn_{25}Ga_{25}$	1134	1116	β (B2)
$Ni_{50}Mn_{30}Ga_{20}$	1119	1103	β (B2)
$Ni_{50}Mn_{40}Ga_{10}$	1080	1068	β (B2)
$Ni_{50}Mn_{50}$	1050	1035	γ (Ni, Mn ss)

Table 3. Thermal analysis data of $Ni_{100-2x}Mn_xGa_x$ alloys

	Liquidus (°C)	Solidus (°C)	Primary Solidification Product
Ni	1455	1455	α(fcc Ni)
$Ni_{80}Mn_{10}Ga_{10}$	1309	1271	α(fcc Ni)
$Ni_{60}Mn_{20}Ga_{20}$	1127	1112	β (B2)
$Ni_{40}Mn_{30}Ga_{30}$	1069	1066	β (B2)
$Ni_{20}Mn_{40}Ga_{40}$	814	795	$Ni(MnGa)_3$
$Mn_{50}Ga_{50}$	845	776	

Table 4 Thermal analysis data of $Ni_{2x}Mn_{100-3x}Ga_x$ alloys

	Liquidus (°C)	Solidus (°C)	Primary Solidification Product
Ni_2Ga	1206	1200	α(fcc Ni)
$Ni_{60}Mn_{10}Ga_{30}$	1170	1165	α'
$Ni_{40}Mn_{40}Ga_{20}$	1048	971	β (B2)
$Ni_{30}Mn_{55}Ga_{15}$	957	948	β (B2)
$Ni_{20}Mn_{70}Ga_{10}$	1054	992	
$Ni_{10}Mn_{85}Ga_5$	1156	1097	Mn (ss)
Mn	1246	1246	

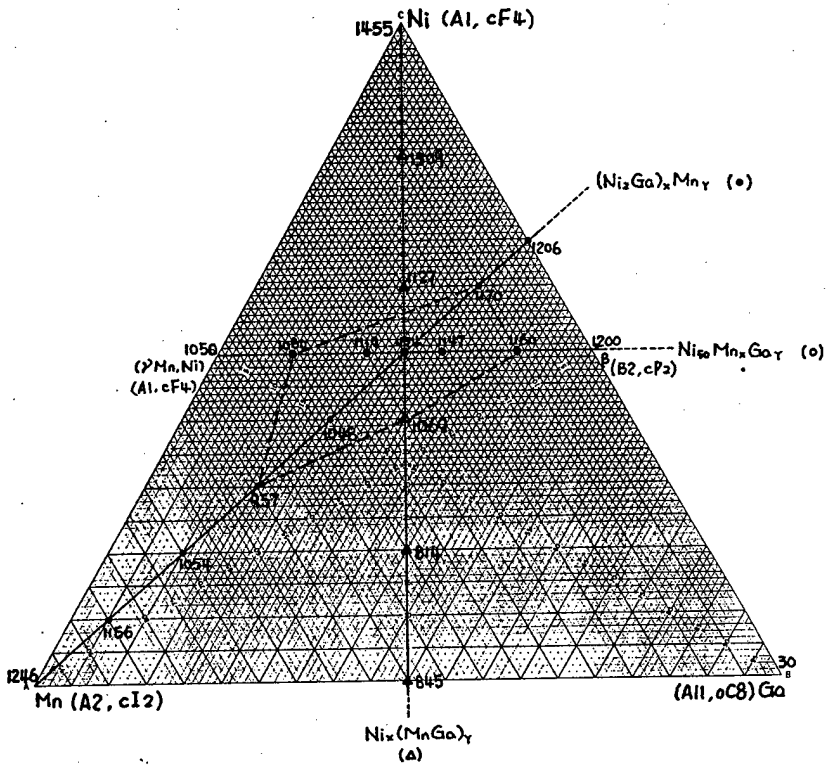

Figure 5 Liquidus projection indicating the approximate compositional range of the primary solidification field of $Ni_{50}Mn_{25}Ga_{25}$.

Compositional Variations during Bridgman Crystal Growth

The compositional profiles for the three Bridgman ingots (standard length, long and short) are shown in Figure 6. In all of the ingots, the Mn concentration increased with solidification distance and the Ni content decreased accordingly. There was also a small decrease in the concentration of Ga along the length of the ingots. These data can be normalized with respect to the solidified distance (fraction solidified), as shown in Figure 7, and the resultant compositional profiles are quite similar. This type of increase (decrease) of composition along the length of the ingots is representative of solidification under a highly convective condition. For the case of a completely mixed liquid, the compositional profile is described by the Schiel equation:

$$C_i = kC_o(1-f_s)^{(k-1)} \qquad (1)$$

Where C_i is the composition of component *i* along the length of the ingot, C_o is the overall composition of the alloy, F_s is the fraction solidified, and k is the partitioning coefficient between solid and liquid. Fitting the data for each element using the above equation yields values for both the overall composition of the ingot and the partitioning coefficient for that element. These values are summarized in Table 5.

First and most notably, the overall composition calculated from the data differs significantly from the nominal starting composition, implying that the solidification did not follow the complete mixing model. While the overall shape of the compositional

profile resembles a completely mixed system, the deviation from complete mixing can be related to three possible factors: 1) partial mixing in the liquid that only approach the extremum condition, 2) a non-constant partitioning coefficient over the solidification range, and 3) weight loss during solidification. The first two conditions are difficult to account for without extensive modeling of the thermo-solutal convection forces and complete determination of the liquid-solid phase equilibria. However, the loss of mass during solidification is a significant problem in Mn-containing alloys. Weight loss data for the three ingots, given in Table 6, shows significant weight loss has occurred during the preparation of these ingots. The severity of weight loss correlates with the difference in the calculated versus nominal compositions. Unfortunately, the effect of weight loss accumulates, as solidification proceeds, and mathematical modeling would be required to fully describe the effect on segregation profile over the length of the ingot. Considering the relative vapor pressures of pure Ni, Mn and Ga, the weight loss is most likely the evaporation of Mn during crystal growth. Assuming the weight loss is solely due to Mn loss, the nominal starting composition can be adjusted for the loss of Mn (see Table 7) and comparing these values to the calculated compositions, some of the deviation in composition can be accounted for.

Second, despite the compositional variability and changing growth conditions in the ingots, the calculated partitioning coefficients for each element are quite similar. As mentioned above, the partitioning coefficients calculated are effective coefficients over the solidification range and do not correspond to the equilibrium partitioning coefficients from the phase diagram. However, the remarkable consistency provides a level of confidence in utilizing theses values for predictive purposes. For example, if a stoichiometric single crystal ($Ni_{50}Mn_{25}Ga_{25}$) is desired, the nominal composition for single crystal growth should be modified by C_i/k_i ($Ni_{47.9}Mn_{27.8}Ga_{23.4}$).

Finally, in terms of minimizing the compositional variations in Bridgman prepared single crystals, the options are unfortunately quite limited. With the level of convective mixing already present in the system only a reduction in convective mixing could lead to a more uniform length profile. This could be accomplished by utilizing higher temperature gradients, which will act a stabilizing force against thermally driven convection, although the anticipated benefits would be small when compared to the solutal driven mixing. On the other hand, these compositional variations present a unique opportunity to determine properties over a range of compositions from the same single crystal sample. Through careful characterization of the composition profile and section of the crystal into individual samples, we will exploit these compositional variations with an on-going collaboration with R. O'Handley, Massachusetts Institute of Technology to investigate the compositional dependency of the Curie temperature, martensite transformation temperatures, magnetic anisotropy and crystal structure parameters.

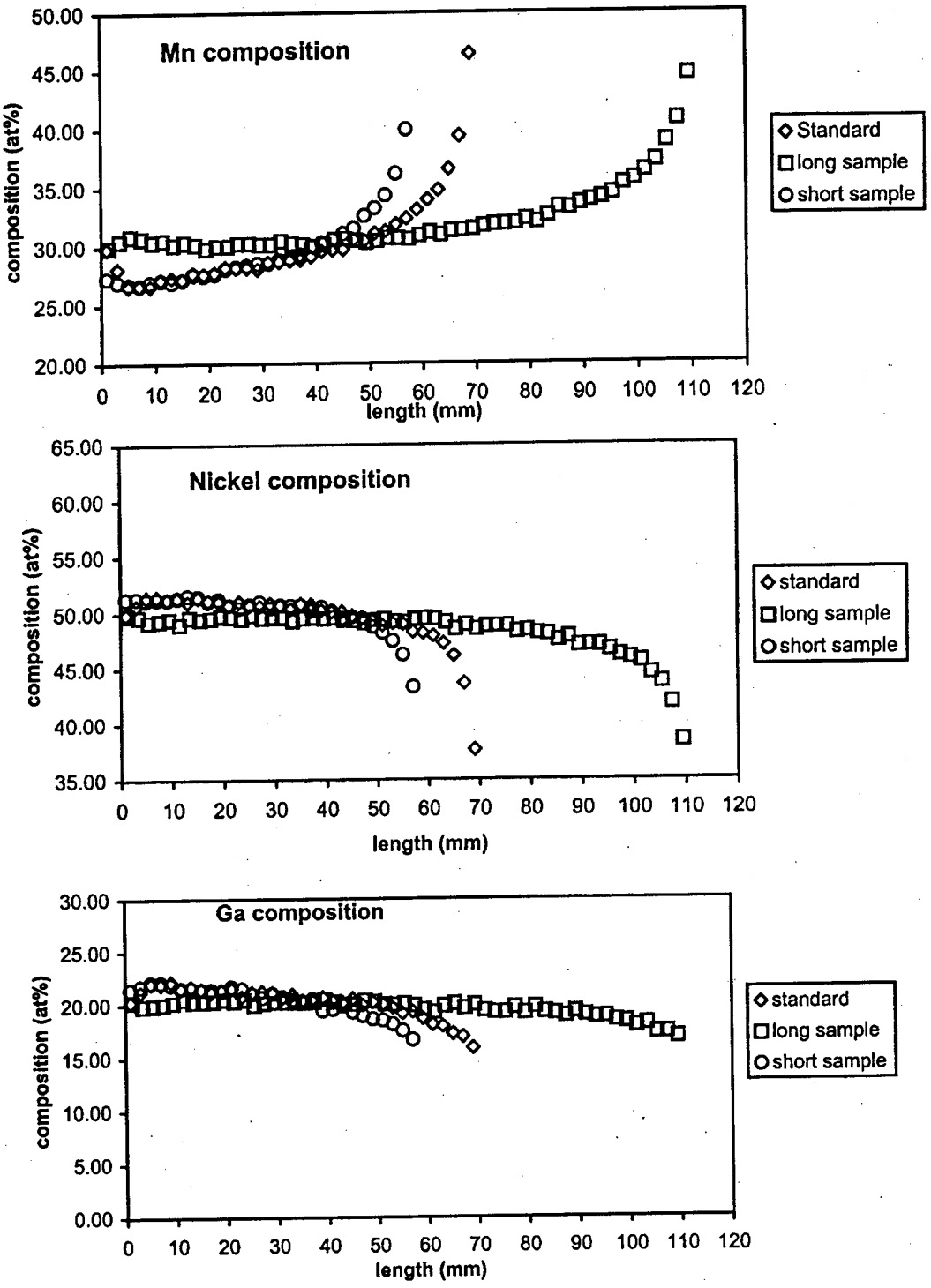

Figure 6 Compositional profile as a function of length measured by EDS for the three Bridgman grown ingots.

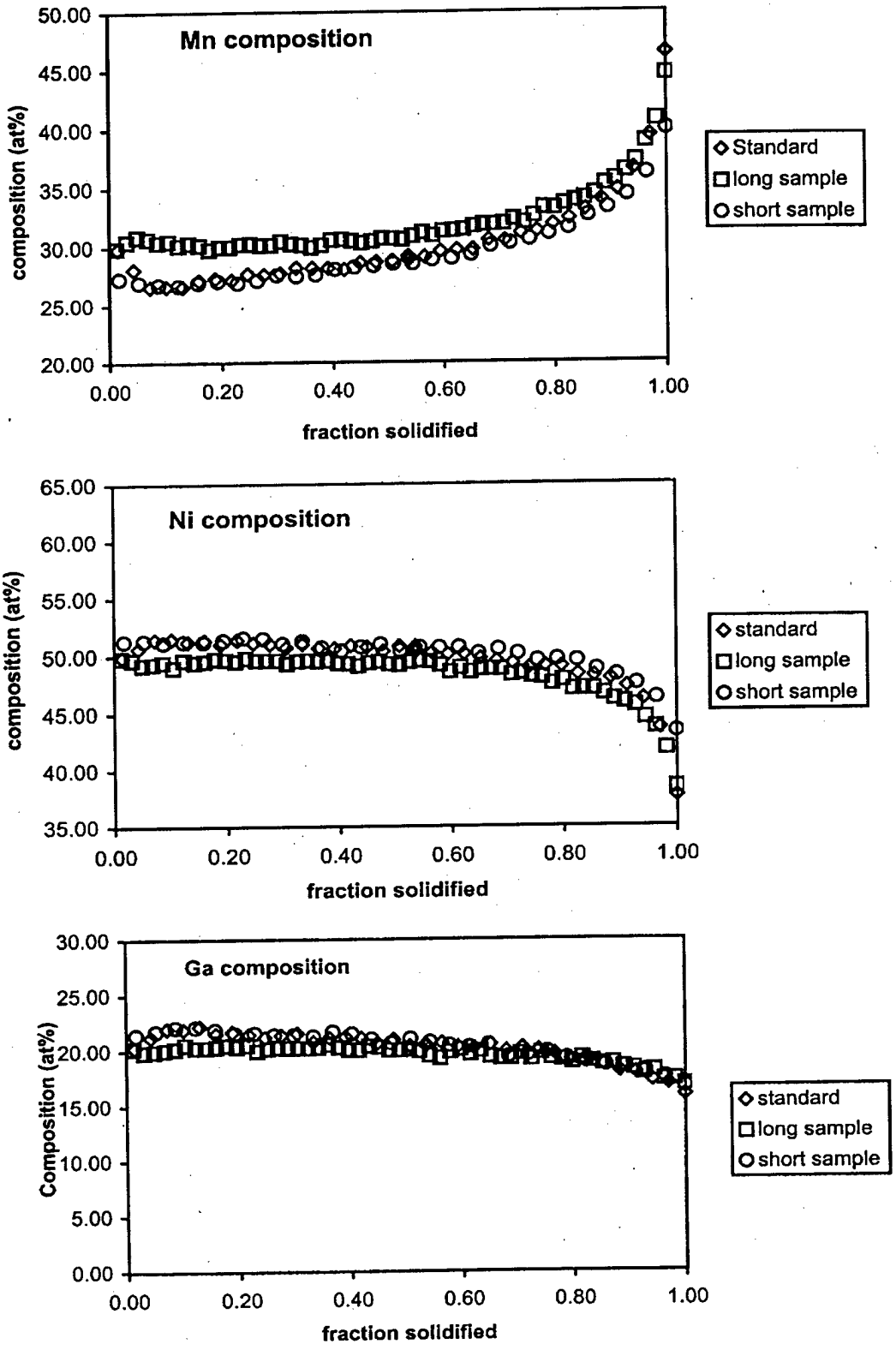

Figure 7 Normalized composition profiles for the three Bridgman ingots.

Table 5 Overall composition and partitioning coefficients for $Ni_{47.4}Mn_{32.1}Ga_{20.5}$ calculated from the Schiel equation fit of the measured compositional profiles.

Ingot	Overall Composition			Partitioning Coefficient		
	Ni	Mn	Ga	Ni	Mn	Ga
Standard	49.8	30.0	20.3	1.041	0.89	1.078
Long	48.5	32.1	19.7	1.048	0.91	1.047
Short	49.9	29.9	20.3	1.042	0.88	1.086
Nominal	47.4	32.1	20.5			

Table 6 Weight loss data from the Bridgman grown ingots.

Ingot Length	Weight In	Weight Out	Weight Loss (%)	Growth Rate (mm/hr)
Standard	93.7 gram	91.7 gram	2.0 gram (2.1%)	2
Long	147.3 gram	146.3 gram	1.0 gram (0.67%)	2
Short	73.8 gram	71.5 gram	2.3 gram (3.1%)	2

Table 7 Comparison of overall composition and the nominal composition adjusted for the weight loss of Mn during growth.

Ingot	Overall Composition			Adjusted Nominal		
	Ni	Mn	Ga	Ni	Mn	Ga
Standard	49.8	30.0	20.3	48.5	30.5	21.0
Long	48.5	32.1	19.7	47.8	31.5	20.7
Short	49.9	29.9	20.3	49.1	29.7	21.2
Nominal	47.4	32.1	20.5			

Crystal Growth by the Czochralski Method (CZ)

Four growth attempts were made during this study to begin to define the operating parameters for growth by the CZ method. The growth parameters and outcomes are detailed in Table 8. The initial two attempts we designed to determine the operating power for the induction heater and to establish diameter control during growth. In both runs, a randomly oriented seed was used and a growth rate of 15 mm/hour. The resultant boules are shown in Figure 8a and 8b and both were found to be polycrystalline down the length. The second two growth attempts utilized an (100) oriented seed and the growth rate was slowed to 10 mm/hr. The general growth procedure is to "dip" the seed into the melt and begin to propagate the seed in a smooth and orderly fashion, ultimately widening the diameter to approximate 12 mm in diameter. Figure 9a shows the resultant boule with the seed crystal still attached (on the right). Characterization of the boule indicated that the ingot started out polycrystalline primarily due to the rather abrupt transition between the seed and the ingot. In this attempt, we allowed the diameter to decrease as the run proceeded and found a single crystal existed at the end of the ingot and therefore characterize the result as mixed. However, because crystal selection occurred due to the reduction of diameter, the single crystal was randomly oriented compared with the seed. A smother transition from seed to ingot was made in the last

growth attempt through better control of the starting parameters as shown in Figure 9b and we were able to demonstrate that the seed crystal could be propagated. Despite this demonstration that the CZ method can be applied to the successful preparation of Ni-Mn-Ga alloys, it is clear that additional processing development is required to reproducibly prepare single crystals.

Table 8 Parameters and results of the Czochralski growth attempts of Ni-Mn-Ga.

Growth run	Growth rate	Seed	Result
1	15	Random	Polycrystal
2	15	Random	Polycrystal
3	10	(100)	Mixed
4	10	(100)	Single crystal

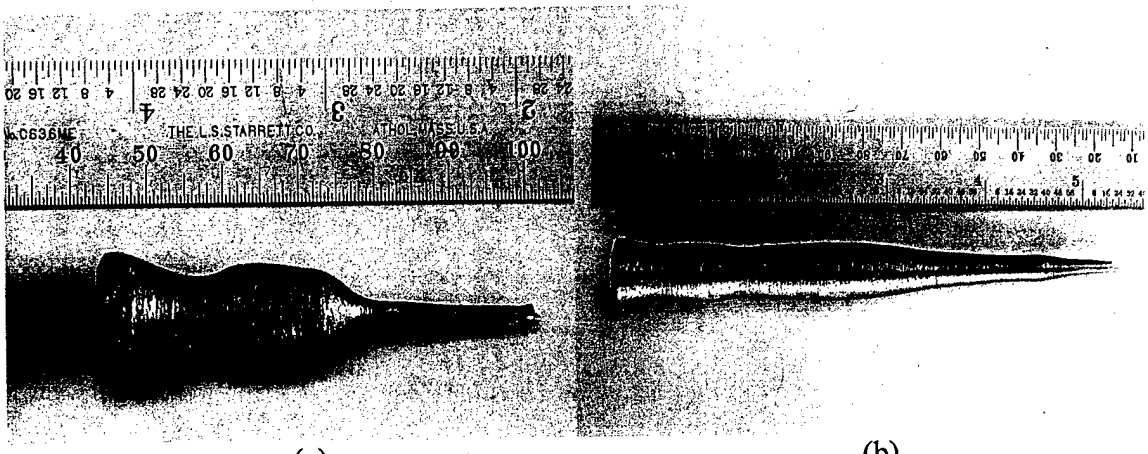

(a) (b)

Figure 8 Czochralski grown boules of $Ni_{47.4}Mn_{32.1}Ga_{20.5}$ using randomly oriented seeds at a growth rate of 15 mm/hr.

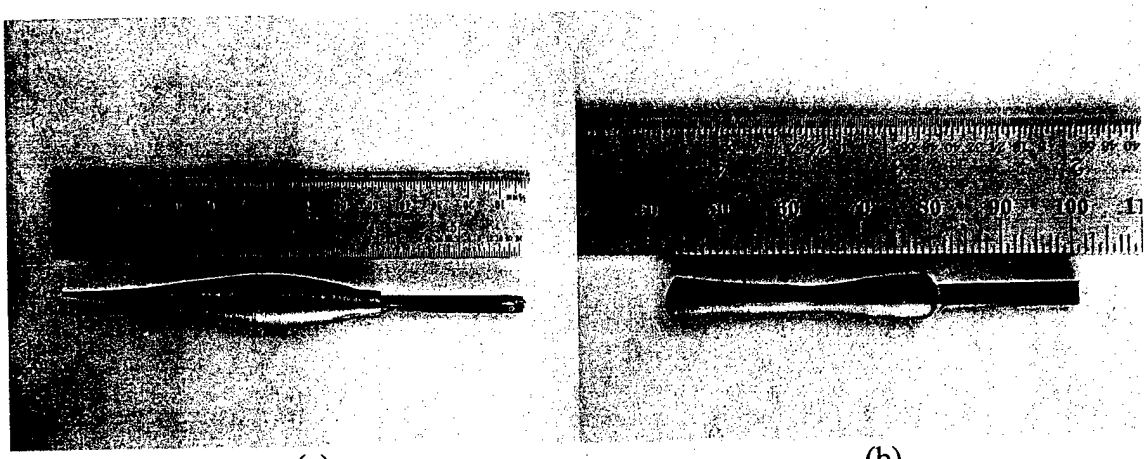

(a) (b)

Figure 9 Czochralski grown boules of $Ni_{47.4}Mn_{32.1}Ga_{20.5}$ using (100) oriented seeds at a growth rate of 10 mm/hr.

Summary

Partial evaluation of the liquidus diagram of Ni-Mn-Ga by thermal analysis and microstructural evaluation has determined that the primary solidification surface for the Heusler alloy phase exists over a wide range of compositions. The primary solidification surface falls modestly in temperature with either increasing Mn or Ga concentrations. The stoichiometric composition, $Ni_{50}Mn_{25}Ga_{25}$, melts incongruently over a temperature range of approximately 18 °C. Furthermore, the solidification temperature range for off-stoichiometric compositions remains small, varying between 10 and 20 °C over the range of compositions examined. The small temperature range of solidification allows for the conditions suitable for crystal growth to be easily established and maintained throughout the crystal growth process for a wide variety of compositions.

Despite the ability to maintain crystal growth conditions, the resultant crystal shows significant variations in compositions as solidification proceeds. In general, the Mn composition increases as the solid grows with an associated decrease in Ni composition. The concentration of Ga is moderately constant throughout most of the growth but shows a modest decreases near the end of the crystals. Analysis of the composition profiles indicated that the compositional changes and hence, the solidification process, is dominated by convective mixing in the liquid during growth. Using the complete mixing model, the effective partitioning coefficients were calculated for each of the elemental constituents and can be utilized to predict the appropriate starting compositions for future growths. In addition, a shift in the overall composition of the alloy was revealed, which correlated with the loss of Mn by evaporation. Initiating measures to control evaporative losses during single crystal preparation will result in greater uniformity of composition between crystal growths.

Finally, preliminary experiments were conducted that demonstrated the feasibility of using the Czochralski technique for the preparation of Ni-Mn-Ga alloys. The ability to propagate a seed crystal during Czochralski growth was also demonstrated. Additional process optimization is required to gain confidence in applying the Czochralski method to the routine preparation of $Ni_{50}Mn_{25}Ga_{25}$ and its alloys.

References

1. V. A. Chernenko, V. V. Kokorin, O. M. Babii and I. K. Zasimchuk, Intermetallics 6 (Elsevier Science Limited, Great Britain), p. 29 (1998).
2. E. Obrado, A. Gonzalez-Comas, L Manosa and A. Planes, J. App. Phys. **83**, 11 (1998)
3. S. J. Murray, M.Farinelli, C. Kanter, J. K. Huang, S. M. Allen and R. C. O'Handley, J. App. Phys. **83**, 11, p. 7297 (1998)
4. R. C. O'Handley, Private communication.